A Standardized Light-Emitting Diode Device for Photoimmunotherapy

Esther de Boer[1,2], Jason M. Warram[1], Elmire Hartmans[3], Peter J. Bremer[4], Ben Bijl[5], Lucia M.A. Crane[1], Wouter B. Nagengast[3], Eben L. Rosenthal[1], and Gooitzen M. van Dam[2]

[1]Department of Surgery, University of Alabama at Birmingham, Birmingham, Alabama; [2]Department of Surgery, University Medical Center Groningen, University of Groningen, Groningen, The Netherlands; [3]Department of Gastroenterology and Hepatology, University Medical Center Groningen, University of Groningen, Groningen, The Netherlands; [4]Philips Consumer Lifestyle, Drachten, The Netherlands; and [5]SurgVision, Heerenveen, The Netherlands

Antibody-based photodynamic therapy—photoimmunotherapy (PIT)—is an ideal modality to improve cancer treatment because of its selective and tumor-specific mode of therapy. Because the use of PIT for cancer treatment is continuing to be described, there is great need to characterize a standardized light source for PIT application. In this work, we designed and manufactured a light-emitting diode (LED)/PIT device and validated the technical feasibility, applicability, safety, and consistency of the system for cancer treatment. **Methods:** To outline the characteristics and photobiologic safety of the LED device, multiple optical measurements were performed in accordance with a photobiologic safety standard. A luciferase-transfected breast cancer cell line (2LMP-Luc) in combination with panitumumab-IRDye 700DX (pan-IR700) was used to validate the in vitro and in vivo performance of our LED device. **Results:** Testing revealed the light source to be safe, easy to use, and independent of illumination and power output (mW cm^{-2}) variations over time. For in vitro studies, an LED dose (2, 4, 6 J cm^{-2})–dependent cytotoxicity was observed using propidium iodide exclusion and annexin V staining. Dose-dependent blebbing was also observed during microscopic analysis. Bioluminescence signals of tumors treated with 0.3 mg of pan-IR700 and 50 J cm^{-2} decreased significantly (>80%) compared with signals of contralateral nontreated sites at 4 h and at 1 d after PIT. **Conclusion:** To our knowledge, a normalized and standardized LED device has not been explicitly described or developed. In this article, we introduce a standardized light source and validate its usability for PIT applications.

Key Words: photoimmunotherapy; standardization; breast cancer

J Nucl Med 2014; 55:1893–1898
DOI: 10.2967/jnumed.114.142299

The ultimate goal of cancer treatment is to obtain complete removal of tumor tissue while minimizing damage to surrounding healthy tissue (*1,2*). Antibody-based photodynamic therapy—that is, photoimmunotherapy (PIT)—can be an ideal modality to improve cancer treatment because of its inherent selectivity for targeting tumors. The application can be used for both initial treatment and eliminating residual microscopic disease during incomplete resection, which is common, for instance, in pancreatic cancer (~75% positive margins) and in locally advanced rectal cancer (~35% positive margins) (*3,4*). PIT uses a nontoxic light-sensitive compound (i.e., a photosensitizer) bound to a tumor-targeting antibody, which can serve as both a diagnostic and a therapeutic agent (*5*). A near-infrared light-emitting diode (LED) is then used to excite the antibody-bound photosensitizer, resulting in cell apoptosis and tumor ablation. Numerous preclinical studies have described the therapeutic potential of PIT in multiple cancer types (*6–8*). Its clinical relevance and application is mainly for superficial, spreading cancers such as skin cancer, melanoma, head and neck cancer, peritoneal metastases (ovarian or colorectal), or microscopic residual after an incomplete resection. However, the scientific standardization, performance, tuning, and validation of a light source for PIT have yet to be developed.

Over the past few years, the use of near-infrared high-power LEDs for PIT applications has become more desirable because of the inexpensive and safe nature of the modality (*6*). However, recent findings have shown that performance can be compromised by illumination variations caused by ineffective heat dissipation, especially considering that the emitted peak wavelength is highly dependent on the core temperature of the LED (*9*). With an increase in core temperature, the emitted peak wavelength will be a higher, less favorable wavelength for photosensitizer excitation of IRDye (LI-COR Biosciences) 700DX, which is commonly used as a preclinical PIT agent (*7,10*).

The primary objective of this study was to design and manufacture a standardized, validated, and safe LED/photodynamic therapy device for IRDye 700DX–based PIT cancer treatment. Our secondary objective was to provide a framework for standardization for future studies in which other newly developed photosensitizers will be evaluated.

The key design parameters of the system developed were to select a light source suitable for excitation of the IRDye 700DX, illuminate a large field of view, obtain sufficient cooling to sustain the light source at the operating temperature, and achieve manageable power output levels (20–200 mW cm^{-2}) for application in various in vitro and in vivo conditions. To reach these functional specifications, a system, hereafter referred to as "LED device," was developed. The device was characterized using the standardized testing environment of domestic appliances, in vitro models, and an in vivo xenograft mouse model of breast cancer.

Received Apr. 28, 2014; revision accepted Aug. 14, 2014.
For correspondence or reprints contact: Gooitzen M. van Dam, Department of Surgery, BA 11, University Medical Center Groningen, Hanzeplein 1, 9713 GZ Groningen, The Netherlands.
E-mail: g.m.van.dam@umcg.nl
Published online Oct. 13, 2014.

MATERIALS AND METHODS

Simulation and Normalization

IRDye 700DX was used as the fluorescent photosensitizer. Illumination was provided by a 690-nm (SMBB690D-1100-02) high-output LED (Marubeni) for fluorochrome excitation. The LED specifications are shown in Table 1.

To ensure homogeneous illumination of the area of interest to be photosensitized in the surgical field, predefined as 5 × 3 cm, with a power output ranging from 20 to 200 mW cm^{-2}, a total of 126 individual LED bulbs were needed. To verify the design of the LED device, shown in Figure 1A, the optical design simulation tool "LightTools" was used (Synopsys).

As demonstrated in Figure 1B, unlike power output, peak wavelength is highly dependent on the LED temperature; therefore, to ensure optimal heat dissipation, 690-nm high-output LEDs (n =126) were mounted on a metal-core printed circuit board attached to the semiconductor-mounting surface of the heat sink (Fischer Elektronik) after exact optical alignment. The special heat sink geometry, consisting of a hollow fin, optimizes the airflow for guaranteed effective heat dissipation and thus will keep the temperature of the light sources within the operating temperatures to stabilize the peak wavelength. The LED system is provided with a tunable LED power supply module (HLG-240H-54B; Meanwell), which enables the user to adjust the emitted power output (mW cm^{-2}).

To outline the capabilities and photobiologic safety of the LED device, multiple optical measurements were performed by Philips Lighting B.V. in accordance with the photobiologic safety standard 62471 of the International Electrotechnical Commission. The LED device was tested for 3 potential hazards by calculating the emission hazard value, which represents the ratio between the emission level and the emission limit. The emission hazard value classifies related risk into 4 groups ranging from no photobiologic hazard (exempt) to hazardous for momentary exposure (risk group 3).

Cell Line and Culture

To validate the in vitro and in vivo performance of our LED system, 2LMP-Luc (a 2× lung metastatic pooled subclone of MDA-MB-231, a gift from Dr. Donald Buchsbaum, University of Alabama), a human breast carcinoma cell line, was used. The 2LMP-Luc cells were previously transformed using the ViraPort retroviral vector (Stratagene). Cells were grown in Dulbecco modified Eagle medium supplemented with 10% fetal bovine serum in tissue culture flasks in a humidified incubator in an atmosphere of 37°C, 95% air, and 5% carbon dioxide.

Panitumumab-IRDye 700 Conjugation

The antibody used, panitumumab (Vectibix; Amgen; 177 kDa), is a fully humanized monoclonal antibody directed specifically to the epidermal growth factor receptor (EGFR). The photosensitizer IRDye 700DX *N*-hydroxysuccinimideester (IR700; 2.0 kDa) was purchased from LI-COR Biosciences. Panitumumab was diluted to 5 mg mL^{-1} in a phosphate buffer solution and incubated with the IR700 for 2 h at room temperature according to the manufacturer's instructions. The mixture was purified with a desalting column (Zeba spin desalting column; Pierce). After purification, the protein concentration and the number of dye molecules per protein were determined by absorption with UV-Vis spectroscopy (NanoDrop-200C; ThermoScientific).

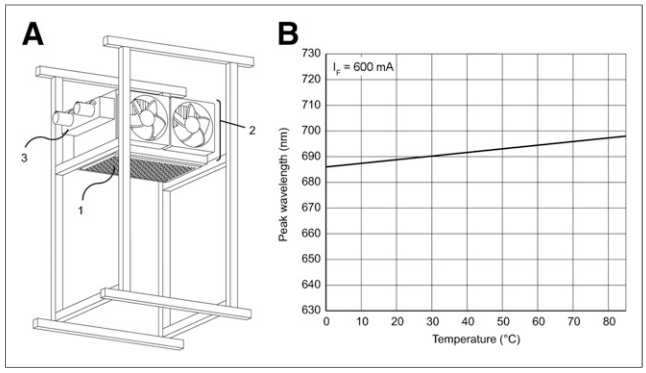

FIGURE 1. Schematic of LED device. (A) Device is provided with multiple LEDs (1) mounted on cooling unit (2). Dimmer (3) allows user to adjust power output to subject specifications. (B) Cooling unit is used to stabilize peak wavelength. I_F = forward current.

To determine the in vitro immunoreactivity of the panitumumab-IRDye 700DX (pan-IR700) after conjugation, a binding assay was performed. Briefly, 3.0 × 10^5 cells were resuspended in phosphate buffer solution containing 5% fetal bovine serum. Pan-IR700 was added (10 μg mL^{-1}) and incubated for 1 h at 37°C. Cells were washed 3 times and resuspended in 200 μL of phosphate buffer solution followed by flow cytometry (Accuri C6; BD Biosciences). Nonspecific binding to the cells was examined by adding a 100-fold excess of cold nonlabeled panitumumab, which was repeated 3 times to obtain a mean fluorescence intensity (MFI; units for MFI are mean photon counts) ± SEM.

In Vitro Cell Viability Assay

To assess PIT effects using the LED device in vitro, cells were harvested and seeded into two 24-well, black-walled plates (Wallac) at 2.0 × 10^5 cells per well for the following treatments: no treatment; PIT at 2, 4, and 6 J cm^{-2}; pan-IR700 only; pan-IR700 and PIT at 2, 4, and 6 J cm^{-2}; pan-IR700 with blocking panitumumab (100-fold excess); and PIT at 2, 4, and 6 J cm^{-2}. Pan-IR700 dose was 10 μg/mL^{-1}. Light microscopy (40×) (IX70; Olympus) was used to visualize morpho-

TABLE 1
System Specifications

Item	Symbol	Condition	Minimum	Typical	Maximum	Unit
Forward voltage	V_F	I_F = 600 mA		2.6	3.0	V
	$V_{F\text{-}PEAK}$	I_{FP} = 2 A		4.0		
Power output	P_O	I_F = 600 mA		490		mW
		I_{FP} = 2 A		1,560		
Peak wavelength	λ_P	I_F = 600 mA	680	690	700	nm
Viewing half angle	^1/2	I_F = 600 mA		±9		Degrees

I_F = forward current; I_{FP} = forward current peak; ^ indicates viewing angle.

logic changes between groups. To determine the cell viability after PIT, cells were harvested and resuspended in 0.1 mL of flow cytometry staining buffer containing propidium iodide (Southern Biotech) and annexin V-FITC (Southern Biotech). The samples were then incubated for 15 min on ice, protected from the light, and analyzed by flow cytometry (Accuri C6).

In Vivo Study Design

Athymic NCr-*nu/nu* female mice (Frederick Cancer Research), aged 5–6 wk, were obtained and housed in accordance with the guidelines of the Institutional Animal Care and Use Committee. All animal experiments were conducted according to the approved protocols of that committee. Mice received a 0.1-mL subcutaneous bilateral flank injection of 2LMP-Luc cells (2×10^6 cells per flank) suspended in fetal bovine serum–free base medium. Tumor growth was monitored by bioluminescence imaging (BLI) using an IVIS 100 imaging system (Caliper Life Sciences) and visual inspection of the flank 2 times a week. At day 21, baseline BLI measurements were collected, and mice were sorted into 2 groups ($n = 3$) based on BLI counts to achieve equal distribution of tumor size. For the treatments, group 1 received 0.1 mg of pan-IR700 (intravenous via tail) 24 h before LED treatment, whereas group 2 received 0.3 mg of pan-IR700. Twenty-four hours after injection, LED treatment was applied to the left and right flank tumors, which received 0 and 50 J cm^{-2}, respectively. Untreated tumor was shielded during contralateral tumor LED treatment. To monitor PIT effects on tumor size, BLI was performed at 4 and 24 h after PIT. Quantitative analysis of total luciferase counts was calculated using tumor-specific ROI analysis performed using integrated instrument software. Therapeutic effect is expressed as the percentage of BLI reduction compared with baseline measurements.

Before LED treatment, all animals were imaged using the Pearl Impulse small-animal imaging aystem (LI-COR Biosciences) in the 700-nm fluorescence emission channel. Average group tumor fluorescence (MFI, defined as total counts divided by the region-of-interest pixel area) was calculated for each group using integrated instrument software.

To evaluate histologic changes after PIT, a standard hematoxylin and eosin–stained microscopic study (serial 20-μm slice sections) was performed. Tumors were surgically removed and fixed in 10% formalin overnight at day 4 after PIT of both the internal negative control and the treated tumor in the same animal.

Statistical Analysis

Data are expressed as mean ± SEM from triplicate experiments unless otherwise indicated. Independent and paired-samples t tests were used to compare the treatment effect with that of the control. For statistical analysis, SPSS version 21.0 was used. A statistically significant difference was indicated by a P value of less than 0.05.

RESULTS

System Characterization

After placing a receiver at various distances from the light source, the peak and average light intensities were simulated (Synopsys). Figure 2A shows that at a distance of 20 cm on an area of 5×3 cm, both the peak and the average power output were 200 mW cm^{-2}. Furthermore, the simulation shows an equal energy distribution (Fig. 2B) at the predefined area of interest (5×3 cm), making this device suitable for in vitro and in vivo applications of PIT. Moreover, the special heat sink geometry was able to keep the temperature at the necessary operating temperature of 50°C (Fig. 2C) to stabilize the peak wavelength over time (Fig. 2D).

To verify the optical design and safety of the LED device, a series of system and safety characterizations was performed. LED system specifications are shown in Table 1. The measured maximum light output was concordant with the simulation and was determined to be 206 mW cm^{-2} with the detector at a distance of 20 cm from the light source. As shown in Table 2, there was no potential hazard to disclose concerning the eye or skin. The emission hazard values for retinal thermal and thermal skin injury were, respectively, 34% and 49% of the emission limit for exempt. Moreover, the emission hazard value for potential hazard caused by infrared exposure to the eye was below the measuring capability range of the system used and therefore far below the emission limit for exempt.

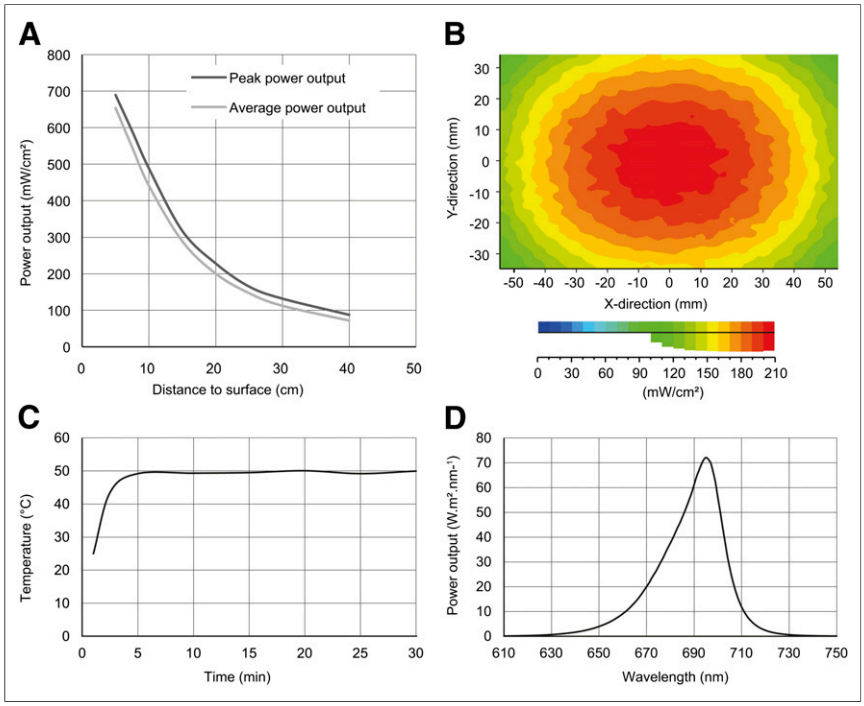

FIGURE 2. Energy distribution, temperature normalization, and wavelength distribution. (A) At 20 cm, both peak and average power output were 200 mW cm^{-2}. (B) Simulation shows equal energy distribution at predefined 5×3 cm area of interest. After 1 min, LED device is capable of stabilizing its core temperature (C) and emitted wavelength distribution (D).

System Validation

Pan-IR700 Conjugate. Conjugation of panitumumab to the fluorescent photosensitizer IRDye 700DX resulted in a dye-to-protein ratio of 1:3 (data not shown). The immunoreactivity of the EGFR-targeting pan-IR700 conjugate was validated in vitro by a binding assay (Fig. 3A). Direct staining of the cell surface epitope of the EGFR 2LMP-Luc cells by the pan-IR700 conjugate caused a significant increase in MFI ($4.6 \times 10^3 \pm 51.8$) compared with the MFI of the control ($0.4 \times 10^3 \pm 11.6$; $P < 0.001$) as determined by flow cytometry. Additionally, after saturating the EGFR antigen-binding sites by adding an excess of native unconjugated panitumumab, nonspecific binding was considered negligible (MFI, $0.7 \times 10^3 \pm 51.8$).

TABLE 2
Hazards

Hazard	Emission level	Emission limit for exempt	Emission level unit	Risk group	Emission hazard value
Retinal thermal	9.49×10^4	2.80×10^5	$W/m^2/sr$	Exempt	0.34
Infrared eye	<2.3	100	W/m^2	Exempt	<0.023
Thermal skin	2.12×10^3	3.5×10^3	W/m^2	Pass	0.49

sr = steradian.

Pan-IR700–Mediated PIT Using Standardized LED System Leads to Rapid Cell Death In Vitro. As shown in Figure 3B, 2, 4, and 6 J cm^{-2} LED exposures of 2LMP-Luc cells incubated with pan-IR700 (10 $\mu g/mL^{-1}$) induced a significantly higher percentage of cell death (32.4% ± 1.4%, 68.5% ± 1.5%, and 89.2% ± 2.4%, respectively) in comparison with untreated control cells (5.7% ± 1.0%: $P < 0.001$). We did not observe significant cytotoxicity without pan-IR700 because of the light exposure of 2 J cm^{-2} (5.3% ± 1.0%), 4 J cm^{-2} (3.9% ± 0.5%), and 6 J cm^{-2} (5.3% ± 0.6%). Treatment with pan-IR700 in the absence of light from the LED device induced no significant cytotoxicity (9.9% ± 0.2%) relative to the PIT-treated groups.

To confirm binding-specific pan-IR700–mediated phototoxicity, 2LMP-Luc cells were incubated with an excess of unlabeled panitumumab to saturate the EGFR target antigen before incubating the cells with the pan-IR700 conjugate (10 $\mu g/mL^{-1}$) and exposure to the light of the LED device. Blocking the EGFR antigen-binding site significantly ($P < 0.001$) reduced the percentage of cytotoxicity at a PIT energy of 2 J cm^{-2} (9.6% ± 0.9%), 4 J cm^{-2} (11.3% ± 0.8%), and 6 J cm^{-2} (11.8% ± 0.9%) after LED illumination. Microscopy studies directly after a 6 J cm^{-2} treatment dose revealed cellular bleb formation and swelling, which are indicators of necrotic cell death induced by PIT (Fig. 3C) (*11*).

Pan-IR700–Mediated PIT by LED System In Vivo. To examine the distribution of pan-IR700 in bilateral 2LMP-Luc tumors, fluorescence imaging was performed at day 1 after intravenous injection of the conjugate. There was a dose-dependent distribution of pan-IR700, with twofold higher MFI signals for a 0.3- versus a 0.1-mg injection (Fig. 4A). Representative fluorescent imaging at the 700-nm channel is shown in Figure 4B. 2LMP-Luc tumors treated with 0.3 mg of pan-IR700 showed a significant decrease in percentage change of BLI signals in treated tumors compared with contralateral nontreated control tumors (Fig. 4C). Figure 4D shows representative BLI signals. No significant decrease in BLI signals was observed in mice that received a 0.1-mg pan-IR700 treatment dose with 50 J cm^{-2} PIT. Histopathologic analysis performed 4 d after PIT revealed that only a small amount of viable 2LMP-Luc cells were present after 0.3 mg of pan-IR700–mediated PIT (Supplemental Fig. 1 [supplemental materials are available at http://jnm.snmjournals.org]).

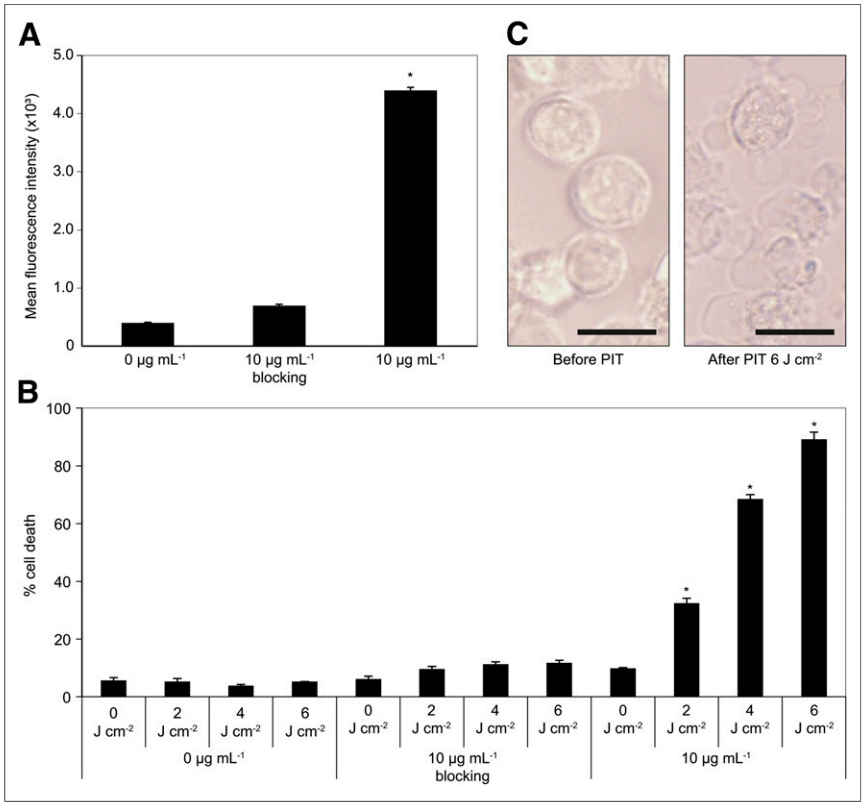

FIGURE 3. Pan-IR700–mediated in vitro PIT for 2LMP-Luc cells. (A) Target-specific binding confirmed by flow cytometer–based immunoreactivity assay. (B) Target-specific cell death in response to pan-IR700–mediated PIT in 2LMP-Luc breast cancer cell line. (C) Microscopic observation of before and directly after 6 J cm^{-2} PIT. Scale bar, 50 μm. Data are mean ± SEM ($n = 3$, *$P < 0.001$ vs. nontreatment control).

DISCUSSION

The use of PIT for the treatment of solid tumors is highly relevant either for superficially located cancer types (primary tumor and locoregional metastases) such as skin cancer, melanoma, head and neck cancer, and colorectal or ovarian peritoneal metastases or for treatment of microscopic residual disease after an incomplete microscopic (R1) or macroscopic (R2) resection. As PIT advances rapidly from preclinical validation to clinical use, a standardized light source is needed. A viable candidate for Food and Drug Administration consideration will be safe, inexpensive, easy to build, robust, reliable, and independent of illumination and temperature variations. To our

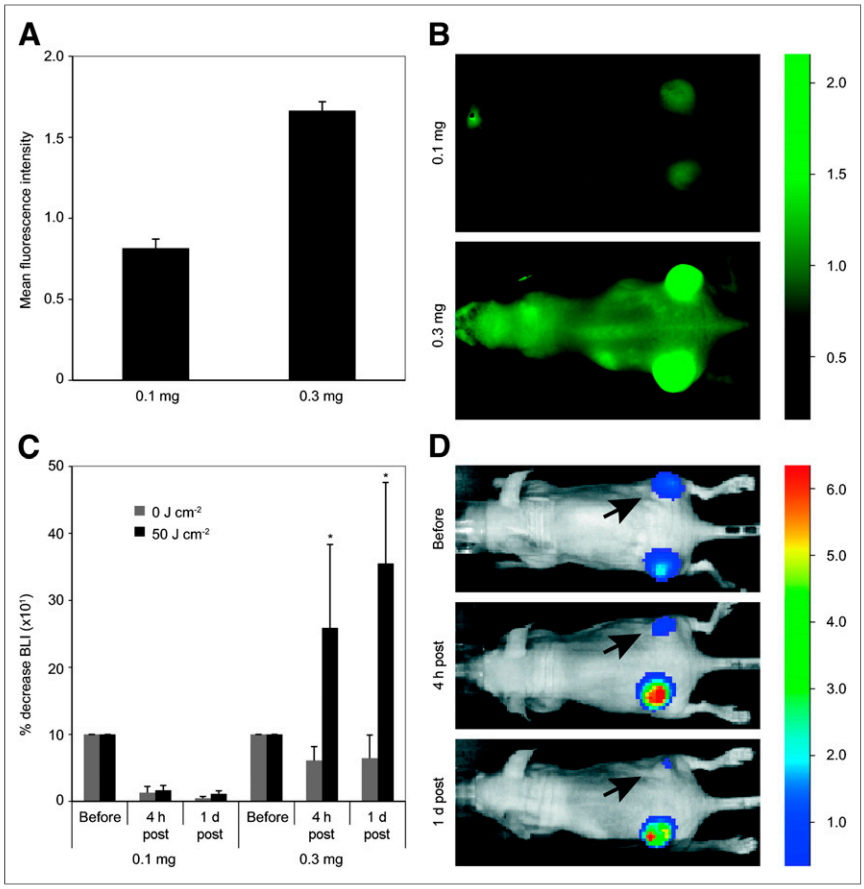

FIGURE 4. Pan-IR700–mediated PIT in vivo. (A) MFI of pan-IR700 in 2LMP-Luc tumors 1 d after injection at 2 different doses of pan-IR700. (B) EGFR-positive 2LMP-Luc (bilateral flank) tumors were clearly visualized 1 d after intravenous pan-IR700 injection of 0.1 mg (top) and 0.3 mg (bottom). (C) BLI signals of tumors treated with 0.3 mg of pan-IR700 (50 J cm^{-2}) decreased significantly compared with BLI signals of contralateral nontreated sites at 4 h and at 1 d after PIT. No significant decrease in BLI signal was observed in tumors treated with 0.1 mg of pan-IR700 (50 J cm^{-2}) compared with contralateral nontreated sites. (D) One day after injection of 0.3 mg of pan-IR700 intravenously, right tumor was exposed to light of LED device (black arrow), whereas left tumor was shielded from light. Data are mean ± SEM (n = 3 mice, $^*P < 0.001$ vs. nonilluminated contralateral control tumor, t test). Colormetric scale in B represents mean fluorescence counts, and colormetric scale in D represents total luciferase counts (×103).

knowledge, a normalized and standardized LED device has never been explicitly described, developed, or validated.

We developed a device appropriate for IR700 excitation that is safe, universal, and standardized. Although high-output laser devices are becoming cheaper, with costs ranging from $10,000 to $25,000, we were able to build a cost-friendly and easy-to-build LED prototype device for less than $1,500. We anticipate that the next generation of devices will be even cheaper because of the reduction in costs of manufacturing larger quantities of components such as LEDs and electronic constituents.

Light in the near-infrared area suffers from low attenuation, with penetration depth up to 1 cm (*12*). Therefore, the skin and eyes of the human body are most at risk when exposed to optical radiation. Although these hazards have been recognized with respect to laser light for many years, their implication in LED light is relatively new, although necessary since the introduction of high-power LEDs (*13*). Hazard testing confirmed that there were no potential hazards concerning the eye or skin to disclose for the device as tested. Moreover, we found that the multiple LEDs mounted on heat exchangers guarantee optimal thermal management of the LEDs, permitting the device to remain within its operating temperatures to deliver a consistent peak wavelength at IR700 optimal peak excitation wavelength (nm).

Consistent with the literature, we showed that target-specific killing by the LED device was achieved in response to a single dose of pan-IR700 and PIT for both in vitro and in vivo studies (*5–7*). Pan-IR700 localized specifically in EGFR-positive 2LMP-Luc tumors, as determined by noninvasive optical imaging. Furthermore, this study shows that target-selective accumulation of pan-IR700 in the EGFR-positive 2LMP-Luc tumors is dose-dependent. An in vivo decrease in tumor growth was confirmed after one dose of 0.3 mg of pan-IR700 followed by a single bolus exposure to light from the LED device (50 J cm^{-2}).

Numerous reports have been published about the clinical implications of fluorescence imaging, providing the surgeon with real-time visualization of tumor deposits to improve resection rates and thus positively influence prognosis. Nevertheless, because of anatomic restraints such as vital tissues, the risk of minimal residual disease remains after an incomplete microscopic (R1) resection or even a macroscopic (R2) irradical resection. PIT can provide clinical applicability not solely for superficial spreading tumors but also as an adjuvant treatment after surgery for irradiating the remaining tumor cavity and its in situ resection margins. We envision the application being used for treatment of localized disease, such as in peritoneal metastases, with a hand-held device, or in an outpatient clinic setting, such as treatment for superficial cutaneous metastases. An advantageous feature of the IR700 photosensitizer is that on excitation it also generates fluorescence. Extending our LED device with a specialized camera system (sensitive charge-coupled device) enables simultaneous registration and processing of the signal for intraoperative real-time imaging combined with PIT capabilities. Moreover, making several technical adjustments may optimize the efficacy of our LED device even more. For example, the bandwidth of the LED presented here is 20 nm. Including additional cutoff filters or selecting LEDs with a narrower bandwidth may increase specificity. Furthermore, further research is necessary to evaluate whether the use of a pulse controller will increase the efficacy of our LED device. We envision that PIT will permit delineation of tumor margins through optical imaging and subsequent light-based phototherapy to eliminate residual microscopic disease, thereby aiding the surgeon in obtaining a more radical resection while preserving as much functionality as possible with minimal collateral damage.

CONCLUSION

To our knowledge, a normalized and standardized LED device has not been explicitly described or developed. In this article, we

have introduced a standardized light source and validated its usability for PIT applications.

DISCLOSURE

The costs of publication of this article were defrayed in part by the payment of page charges. Therefore, and solely to indicate this fact, this article is hereby marked "advertisement" in accordance with 18 USC section 1734. In addition to institutional funding provided by the University Medical Center Groningen and the University of Alabama at Birmingham, this work was supported by Stichting Professor Michaël-van Vloten Fonds. No other potential conflict of interest relevant to this article was reported.

ACKNOWLEDGMENTS

We thank Peter Tuinier for his input regarding engineering and the drawing of the LED device and Sikke Lautenbach (Led Factory) for assemblage and data collection.

REFERENCES

1. Hickey R, Vouche M, Sze DY, et al. Cancer concepts and principles: primer for the interventional oncologist—part I. *J Vasc Interv Radiol.* 2013;24:1157–1164.
2. Hickey R, Vouche M, Sze DY, et al. Cancer concepts and principles: primer for the interventional oncologist—part II. *J Vasc Interv Radiol.* 2013;24:1167–1188.
3. Verbeke CS, Gladhaug IP. Resection margin involvement and tumour origin in pancreatic head cancer. *Br J Surg.* 2012;99:1036–1049.
4. Phang PT, Kennecke H, McGahan CE, Macfarlane J, McGregor G, Hay JH. Predictors of positive radial margin status in a population-based cohort of patients with rectal cancer. *Curr Oncol.* 2008;15:98–103.
5. van Dongen GA, Visser GW, Vrouenraets MB. Photosensitizer-antibody conjugates for detection and therapy of cancer. *Adv Drug Deliv Rev.* 2004;56:31–52.
6. Mitsunaga M, Ogawa M, Kosaka N, Rosenblum LT, Choyke PL, Kobayashi H. Cancer cell-selective in vivo near infrared photoimmunotherapy targeting specific membrane molecules. *Nat Med.* 2011;17:1685–1691.
7. Mitsunaga M, Nakajima T, Sano K, Kramer-Marek G, Choyke PL, Kobayashi H. Immediate in vivo target-specific cancer cell death after near infrared photoimmunotherapy [abstract]. *BMC Cancer.* 2012;12:345.
8. Nakajima T, Sano K, Choyke PL, Kobayashi H. Improving the efficacy of photoimmunotherapy (PIT) using a cocktail of antibody conjugates in a multiple antigen tumor model. *Theranostics.* 2013;3:357–365.
9. Yung KC, Liem H, Choy HS. Heat dissipation performance of a high-brightness LED package assembly using high-thermal conductivity filler. *Appl Opt.* 2013;52:8484–8493.
10. Ding TP, Guo WL, Cui BF, Yin F, Cui DS, Yan WW. The effect of temperature on the PL spectra of high power LED. *Guang Pu Xue Yu Guang Pu Fen Xi.* 2011;31:1450–1453.
11. Kang B, Austin LA, El-Sayed MA. Observing real-time molecular event dynamics of apoptosis in living cancer cells using nuclear-targeted plasmonically enhanced Raman nanoprobes. *ACS Nano.* 2014;8:4883–4892.
12. Ntziachristos V, Yoo JS, van Dam GM. Current concepts and future perspectives on surgical optical imaging in cancer [abstract]. *J Biomed Opt.* 2010;15:066024.
13. Takac S, Stojanovic S. Classification of laser irradiation and safety measures. *Med Pregl.* 1998;51:415–418.